Elastomer
Vol. 34, No. 4, pp. 321~331 (1999)

Dynamic Optimization of a Tire Curing Process for Product Quality

In-Su Han, Chang-Bock Chung†, and Sung-Ju Kang*
Faculty of Applied Chemistry College of Engineering Chonnam National University Kwangju 500-757, Korea
**Dept. of Chemical Engineering Colege of Engineering College of Engineering Chonnam National University*
Kwangju 500-757, Korea
(Received July 31, 1999)

제품품질을 위한 타이어 가황공정의 동적 최적화

한 인 수 · 정 창 복† · 강 성 주*
전남대학교 공과대학 응용화학부, *화학공학과
(1999년 7월 31일 접수)

ABSTRACT : The curing process is the final step in tire manufacturing whereby a green tire built from layers of rubber compounds is formed to the desired shape and the compounds are converted to a strong, elastic materials to meet tire performance needs under elevated pressure and temperature in a press. A numerical optimization procedure was developed to improve product quality in a tire curing process. First, a dynamic constrained optimization problem was formulated to determine the optimal condition of the supplied cure media during a curing process. The objective function is subject to an equality constraint representing the process model that describes the heat transfer and cures kinetic phenomena in a cure press and is subject to inequality constraints representing temperature limits imposed on cure media. Then, the optimization problem was solved to determine optimal condition of the supplied cure media for a tire using the complex algorithm along with a finite element model solver.

요 약 : 타이어 가황공정(curing process)은 타이어 제조를 위한 최종공정으로 여러 개의 고무배합물 층으로부터 성형된 그린타이어(green tire)를 가황기(mold)내에서 고압/고온 조건하에 유지시킴으로써 원하는 형상을 얻게 하고, 아울러 각 고무배합물이 고탄성을 갖도록 물성을 변화시키는 공정이다. 본 연구에서는 타이어 품질의 향상을 위해 가황공정을 수치적으로 최적화하는 기법을 개발하였다. 먼저, 가황공정 중 가황매체(cure media)의 최적공급 조건을 결정하기 위해 제약조건을 갖는 동적최적화문제(dynamic constrained optimization problem)로 정형화 하였다. 즉, 가황기 내의 전열 및 가황 반응 현상을 묘사하는 공정모델로 표현되는 등위제약조건(equality constraint)과 가황매체가 갖는 온도의 한계를 표현하는 부등위제약조건(inequality constraint) 아래 목적함수를 최적화 시켰다. 다음, 공급되는 가황매체의 최적조건을 결정하기 위해 구성된 최적화문제를 유한요소법(FEM)

†대표저자(*e-mail : chungcb@chonnam.chonnam.ac.kr*)

과 complex 알고리즘을 적용하여 풀었다.

Keywords : tire curing process, dynamic optimization, finite element method, cure kinetics, cure step.

I. Introduction

Tire curing process is one of the most important steps in tire manufacturing whereby a green tire built from layers of rubber compounds is formed to the desired shape and the compounds are converted from a weak fluid material to a strong, elastic solid one to meet tire performance needs. The curing process usually takes place under elevated pressure and temperature in a press (also called mold). In the press, heat is transferred to the green tire from the mold and the bladder, which are kept at higher temperatures by circulated cure media like steam, nitrogen gas, hot water, etc. The major operating variables of the curing process are the conditions of the supplied cure media, which are to be varied according to prescribed *cure steps*. It is desirable to adjust the temperature and pressure of the cure media as a function of time so that the rubber compounds may attain specified levels of the state of cure (SOC). But in practice the distributed nature of heat transfer mechanism makes it difficult to have every compound reach the respective target level. Inside layers of a tire cannot be fully cured without causing the over-cure of surface layers and the consequent reversion of vulcanized cross-links. Accordingly, there arises a need to make trade-offs between different parts of the tire with respect to the attainable SOC levels and other product quality measures like temperature history during cure.

To optimize the cure steps for different compounds of various dimensions requires proper evaluation of the time-dependent temperature distribution in the tires. The conventional method to set up cure steps is to directly measure the temperature-time profiles using the thermocouples inserted into various parts of a green tire and then to convert the measured profiles to the SOC on the basis of some assumed cure kinetics.[1] This procedure has to be repeated several times with the cure steps altered each time until reasonable trade-offs are made. Thus, there has been a need to develop an alternative method that would replace the costly and time-consuming thermocouple experiments.

The purpose of this study is to develop a systematic optimization procedure for determining optimal cure steps for product quality in a tire curing process. A dynamic optimization problem is formulated to optimize a measure of product quality in terms of the final state of cure and the temperature history at selected points in a tire. The optimization is carried out with the process model and the temperature limits of cure media as constraints. The time-varying profile of cure media temperature is discretized using B-splines2. Then the optimization problem is solved using the complex algorithm along with a finite element model solver. Numerical simulations are presented to demonstrate the procedure of determining the optimal cure steps for a tire.

II. Formulation of a Dynamic Optimization Problem

1. Cure Optimization Problem

The state of cure represents the single most important measure of tire product quality as far as the curing process is concerned. The optimal product quality postulated in this study is to make the final states of cure of the selected rubber compounds approach their respective target values in a coordinated fashion. Another factor that affects the product quality is the temperature history experienced by heat-sensitive materials within tire during the cure: the temperature of composite layers should not exceed respective prescribed limits in order not to cause the deterioration of adhesion force. Now the problem of determining optimal cure steps for product quality in a curing process can be formulated as an optimization problem as follows:

$$\underset{T_m(t)}{Minimize}\ J=\frac{1}{n}\sum_{i=1}^{n}(x_i(t_f)-x_i^{set})^2 + \frac{r}{m}\sum_{j=1}^{m}\int_0^{t_f}[\max(T_j(t)-T_j^{set},\ 0)]^2\,dt \quad (1)$$

$$\text{Subject to } f(x,\ T,\ T_m(t))=0 \ for\ 0\le t\le t_f \quad (2)$$

$$T_{m,l}\le T_m(t)\le T_{m,u}\ for\ 0\le t\le t_h \quad (3)$$

where,

J = objective function

r = weight factor

x = state of cure

n = number of state of cure observation points

x_i^{set} = desired state of cure at observation point i

T = Temperature

m = number of temperature observation points

T_j^{set} = upper temperature limit at observation point j

$f(x,\ T,\ T_m(T))$ = process model

$T_m(t)$ = cure steps (temperature profile of cure media)

$T_{m,l}$ = lower limit for $T_m(t)$

$T_{m,u}$ = upper limit for $T_m(t)$

f_f = final time

t_h = curing time(mold opening time)

The equality constraint of equation (2) represents the process model which relates the state of cure and temperature to the cure media temperature, and the inequality constraints of equation (3) represents the operational limits of cure media temperature. In practice, the SOC observation points are mainly placed in the parts of a tire where either overcure or undercure is likely to occur while the temperature observation points are placed onto thermally sensitive layers like belt, steel and nylon chafer, bead wrap, and ply. The weight factor r provides additional flexibility to adjust relative significance between the two measures of product quality.

2. Dynamic Model for a Tire Curing Process

The process model f in equation (2) consists of heat transfer mechanisms and curing reaction kinetics. First, heat transfer taking place in a tire curing process can be described by the following second-order parabolic partial differential equations:[3]

$$\rho C_P \frac{\partial T}{\partial t} = \Delta \cdot (k \Delta T) + Q \ in \ \Omega \times (0, t_f) \quad (4)$$

$$\text{where, } Q = \rho(-\Delta H)\frac{dx}{dt} \quad (5)$$

$$I.C. : T(z, 0) = T_0(z) \ in \ \Omega \quad (6)$$

$$B.C. : T(z, t) = \hat{T}(t) \ on \ \partial\Omega_1 \quad (7)$$

$$-k\frac{\partial T}{\partial n} = h(T - T_a(t)) \ on \ \partial\Omega_2 \quad (8)$$

In the above equations, ρ denotes the density, C_P the specific heat, k the thermal conductivity, h the convective heat transfer coefficient. Q represents the rate of heat generation which depends on the rate (dx/dt) and heat (ΔH) of vulcanization of rubber compounds. Ω is the analysis domain in the spaces of z with the boundary segments $\partial\Omega_1$ and $\partial\Omega_2$ where an essential and a natural boundary condition is prescribed, respectively.

The heat equations in equations (4)-(8) have several characteristics associated with tire curing processes. First, since the cure reactions of rubber compounds take place not only during the heating stage in a press but also during the cooling stage out of the press, one must solve the equations in two separate stages with the change of domain Ω in-between. Next, the equations are nonlinear due to the dependence of the rubber compound properties on temperature and the state of cure. Finally, since the conditions of the cure media supplied to a bladder side or a mold side are changing according to predefined cure steps, it is necessary to model such conditions in terms of time-varying boundary conditions as shown in equations (7) and (8).

The other component comprising the process model f is the kinetic model for the cure reaction which is a process of chemically producing network junctures by the insertion of cross-links between polymer chains. The state of cure denotes the extent of the reaction and is determined by measuring the rubber properties dependent on the cross-link density. The most popular and practical method of measuring SOC is based on rheometry whereby time-varying torque required for maintaining a given dynamic strain on a vulcanizing rubber specimen is recorded.

In this study, a cure kinetic model proposed earlier by the authors[4] is used to explain the reversion and the induction period that are commonly found in the vulcanization of rubber compounds. The model postulates a reaction mechanism with the three reaction paths as shown in Fig. 1. Where s denotes the current amount of sulfur, c_1 the strong and stable cross-links, c_2 the weak and unstable cross-links. Once destroyed, the weak cross-links cannot participate in the vulcanization again, thus being responsible for cure reversion.

After defining the amount of each species against the initial amount of sulfur s_0

$$\tilde{s} = \frac{s}{s_0}, \ x_1 = \frac{c_1}{s_0}, \ x_2 = \frac{c_2}{s_0}, \quad (9)$$

one can easily obtain the following rate equations:

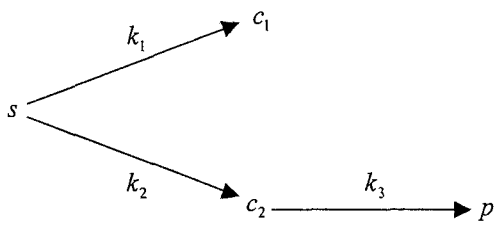

Fig. 1. Schematic of the cure reaction paths.

$$\left.\begin{array}{ll} \tilde{s}=0,\ x_1=x_2=0 & \text{for } t<t_i \\ \dfrac{d\tilde{s}}{dt}=-(k_1+k_2)\tilde{s} & \\ \dfrac{dx_1}{dt}=k_1\tilde{s} & \text{for } t\geq t_i \\ \dfrac{dx_2}{dt}=k_2\tilde{s}-k_3x_2 & \end{array}\right\} \quad (10)$$

where t_i denotes the induction period. Now the sum $x=x_1+x_2$ represents the state of cure corresponding to both the strong and weak cross-links. The temperature dependence of kinetic parameters are described by the following Arrhenius type equations:

$$k_i=k_{i0}\exp[-E_i/RT(t)],\ i=1,2,3 \quad (11)$$

$$t_i=t_{i0}\exp[-E_{ti}/RT(t)] \quad (12)$$

3. B-Spline Representation of Cure Steps

The optimization problem stated in equations (1)-(3) is an optimal control problem in nature where the *control function* $T_m(t)$ that minimizes the given *objective functional* J is to be found. The solution of an optimal control problem is usually constructed on the basis of the Pontryagin's minimum principle[5] derived from variational calculus. But it is simply impractical to apply the minimum principle to the distributed parameter system like ours because the partial differential heat transfer equation will result in too many state equations to handle even after rough, approximate discretization. An alternative method will be to represent the control function *a priori* as a linear combination of appropriate basis functions. This *control vector parameterization* renders the optimization problem finite-dimensional where a vector of coefficients that minimize the *objective function* is to be found, and thus allows the use of well-established multivariate optimization techniques no matter how complex the process model may be. In this study the control vector $T_m(t)$is parameterized using B-splines as follows:

$$T_m(t)=\sum_{i=1}^{N}\theta_iB_i(t) \quad (13)$$

Ⅲ. Numerical Algorithms

Our numerical algorithm for solving the optimization problem in equations (1)-(3) using the B-splines parameterization of equation (13) consists of two major modules: 1) a solver that computes the solutions of the heat transfer equation and the cure rate model for a given vector θ of B-spline coefficients, and 2) an optimization algorithm that finds the optimal vector that θ^* minimizes the objective function J.

The solver for the process model was constructed on the basis of the finite element method (FEM).[6,7] The numerical algorithm, code development and execution procedure are presented in detail in our previous study[8] which aimed at developing a rigorous dynamic simulator for tire curing processes. A major change introduced in the present study is the fourth-order Runge-Kutta method for solving the reversion type cure model of equation (10) that replaces the non-reversion type cure kinetics employed in the previous study[8].

The constrained optimization problem with

respect to θ was solved using the complex method[9] which extends the simplex method to problems with inequality constraints. The complex method is a direct method that only uses the function values and does not require the gradients of an objective function. Although direct methods are generally believed to be less efficient than gradient-based methods like quasi-Newton or successive quadratic programming methods, the complex method was found to outperform the latter methods for our problem. This is because the objective function J is not differentiable at some values of θ due to the induction period t_i in the cure kinetic model and thus the gradient-based methods fail to provide reliable improvement of θ in the neighborhood of such singular points.

IV. Estimation of Rubber Compound Properties

The three thermal properties (k, ρ, C_p) of rubber compounds appearing in equation (4) are dependent on temperature and/or the SOC. First, these properties of rubber compounds were measured at several temperature points using the devices listed in Table 1. Then, the coefficients of the properties were determined from regression of the experimental values assuming that these properties have linear dependencies on the temperature and/or the SOC as shown in Table 1. The values or the regressed coefficients of the properties of rubber compounds comprising a tire were determined in our previous work.[8]

The frequency factors and activation energies appearing in equations (11) and (12) were estimated on the basis of rheometry experiments. The measured torque curves were related to the SOC profiles as follows:

$$\Gamma(t)=\Gamma_0+(\Gamma_m-\Gamma_0)\,x(t) \tag{14}$$

where Γ_0 denotes the initial torque, and Γ_m the hypothetical maximum torque that would be obtained at the fully cured state. First, the least-squares method was used to find the three rate constants (k_1, k_2, k_3) and the induction period (t_i) along with Γ_0 and Γ_m that best fit an isothermal rheometer curve:

$$\underset{\Psi}{Minimize}\; g=\sum_{j=1}^{M}\left[\Gamma_j(\Psi)-\Gamma_j^{obs}\right]^2 \tag{15}$$

Table 1. Measuring Devices, Conditions, and Dependency Expressions for Rubber Compound Properties

Property	Device	Condition	Dependency expression
Rheometer curve	Monsanto MDR-2000 and R-100	At 130℃, 145℃, and 160℃	–
Thermal conductivity(k)	Thermal conductivity tester (Model TCHM-LT)	At 4 temperatures between 50℃ – 100℃	$k(T)=a+bT$
Density(ρ)	Mettler AE 240	At room temperature	$\rho(x)=(1-x)\rho_u+x\rho_c$
Specific heat C_p	Perkin Elmer DSC-7	Range : 20℃ – 300℃ Scaling rate : 20℃/min	$C_p(T,x)=(1-x)C_{pu}(T)+xC_{pc}(T)$ where $C_{pu}(T)=a_u+b_uT$ $C_{pc}(T)=a_c+b_cT$
Heat of vulcanization($-\Delta H$)	Perkin Elmer DSC-7	〃	–

※ the subscript u indicates and "uncured" state ($x=0$) and c indicates a "fully cured" state ($x=1$)

Table 2. Cure Kinetic Parameters of the Rubber Compounds for a Tire

Compound No.	$k_1(\text{min}^{-1})$	$k_2(\text{min}^{-1})$	$k_3(\text{min}^{-1})$	E_1 (cal/mole)	E_2 (cal/mole)	E_3 (cal/mole)	t_{i0}(min)	E_{ti} (cal/mole)
1	3.90037×10^{7}	1.28714×10^{13}	7.28365×10^{10}	16268.72	27300.62	23645.98	6.22571×10^{-13}	24970.34
2	4.19658×10^{11}	1.97614×10^{8}	2.53045×10^{20}	23813.58	17643.10	42326.41	5.69591×10^{-12}	23171.81
3	1.03245×10^{8}	1.03325×10^{13}	3.70585×10^{11}	17103.87	26998.55	25578.70	7.36992×10^{-14}	26810.24
4	1.03245×10^{8}	1.03325×10^{13}	3.70585×10^{11}	17103.87	26998.55	25578.70	7.36992×10^{-14}	26810.24
5	4.19658×10^{11}	1.97614×10^{8}	2.53045×10^{20}	23813.58	17643.10	42326.41	5.69591×10^{-12}	23171.81
6	1.36842×10^{4}	4.74034×10^{13}	4.80945×10^{14}	9695.75	28637.13	29912.58	7.86404×10^{-10}	18866.59
7	3.91349×10^{10}	5.94700×10^{9}	2.89075×10^{19}	22165.80	20434.78	41555.77	1.04358×10^{-12}	24431.78
8	1.02745×10^{11}	8.75372×10^{10}	1.83135×10^{16}	22894.43	22752.03	34726.80	3.66778×10^{-11}	20974.18
9	5.25279×10^{10}	2.49444×10^{7}	1.21786×10^{23}	22412.35	16089.11	47747.09	1.50666×10^{-11}	22103.53
10	1.02745×10^{11}	8.75372×10^{10}	1.83135×10^{16}	22894.43	22752.03	34726.80	3.66778×10^{-11}	20974.18
11	3.91349×10^{10}	5.94700×10^{9}	2.89076×10^{19}	22165.80	20434.78	41555.77	1.04358×10^{-12}	24431.78
12	5.12783×10^{16}	1.04109×10^{5}	4.48183×10^{28}	33796.79	11709.37	58607.00	1.80519×10^{-11}	22048.99
13	2.71568×10^{7}	8.62092×10^{10}	4.32487×10^{09}	16447.02	23233.00	20173.60	1.61173×10^{-11}	22132.94
14	1.39709×10^{13}	2.89628×10^{4}	2.47935×10^{40}	27338.14	10888.27	81702.84	4.40583×10^{-12}	23167.89
15	3.91349×10^{10}	5.94700×10^{9}	2.89076×10^{19}	22165.80	20434.78	41555.77	1.04358×10^{-12}	24431.78
16	3.67054×10^{14}	4.03045	0	29830.58	19672.84	0	2.67236×10^{-11}	22134.83

where Ψ denotes estimated parameters: k_1, k_2, k_3, Γ_0, Γ_m, and t_i. Minimization of equation (15) was carried out using the MINPACK-2 routine.[10] This nonlinear regression step was repeated for several temperatures. Then from the Arrhenius plot of the estimated k_i's and t_i's vs. temperature, the frequency factor and the activation energy of each parameter were determined. Table 2 lists the estimated cure kinetic parameters for the 16 rubber compounds comprising a tire.

V. Numerical Simulations and Discussions

The optimization algorithm was applied to the problem of determining optimal cure steps for a tire in a dome type press. Fig. 2 shows a quarter cross section of the axisymmetric press assembly and the structure of the layers in the tire. Fig. 3

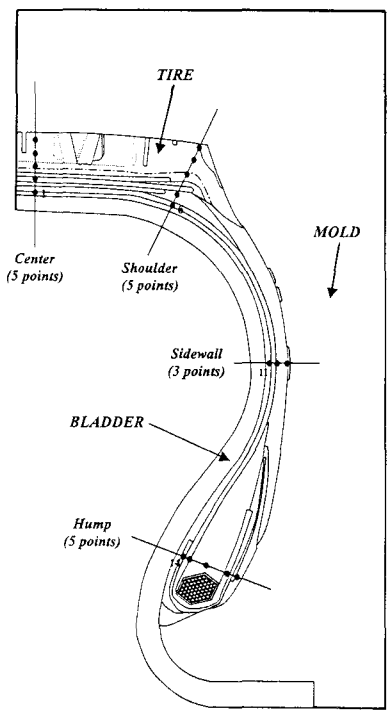

Fig. 2. A quarter cross section of the cure press.

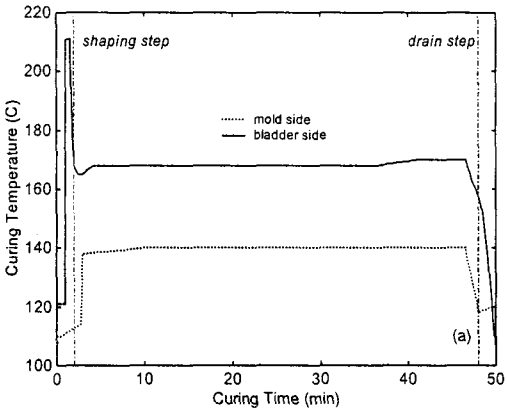

Fig. 3. Temperature profiles of the cure media during a pilot test for a tire

shows the time-varying temperatures of the cure media supplied to the dome side and the bladder side, respectively, during a pilot test for determining the cure steps for the tire.[8] The initial two minute period represents a shaping period during which the green tire is pressed against the mold by high pressure steam to ensure the correct tread pattern to be realized. The cure media are gradually drained with the temperature falling to 104℃ for several minutes before the mold is open at t_h. Here the optimal curing problem is assumed to consist of determining the optimal temperature profile of the bladder side cure media after the shaping period until the mold opening time.

The objective function formulated in equation (1) was used in our simulation with $n=18$ and $m=30$. The 18 SOC observation points were assigned to the center(5), shoulder(5), sidewall(3), and hump(5) section, respectively, with x_i^{set} uniformly set equal to 1 (see Fig. 2). Six temperature observation points were placed evenly along each of the following heat-sensitive layers:belt(145℃), steel chafer(145℃), bead wrap/bundle (145℃),

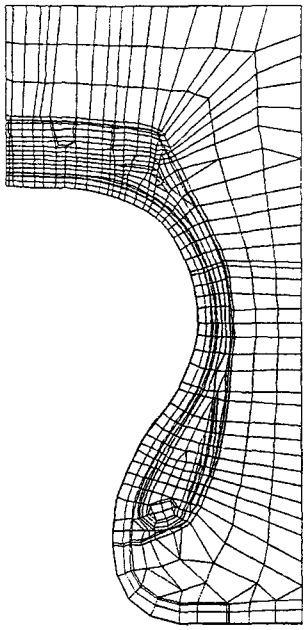

Fig. 4. Finite element mesh generated for the tire cure press.

nylon chafer (193℃), and ply (152℃), where the temperatures in parentheses denote the temperature limits for respective layers. The temperature of the bladder side cure media was assumed to be adjustable between 100 and 212℃.

To solve the heat transfer model shown in equations (4)-(8), a finite element mesh was generated for the analysis domain shown in Fig. 2. Fig. 4 depicts a finite element mesh which consists of 1001 axisymmetric quadrilateral elements, 36 triangular elements, 1072 nodes, and 18 materials. At the cooling stage after the mold is open, the mesh for the tire section only was retained for solving the model until t_f=130min. The cubic splines were used to represent the cure media temperature $T_m(t)$. It should be noticed, however, that θ_1 and θ_6 are constrained at 168 and 104℃, respectively, during optimization because of the

Table 3. Results of the Cure Optimization Runs

t_h(min)	J_x(−)	J_T(℃²min)	J(−)	# of function evaluations
50(Pilot)	1.8572×10^{-2}	9.6296×10^{1}	9.6315×10^{1}	−
50(Optimal)	1.1781×10^{-2}	2.0638×10^{-7}	1.1781×10^{-2}	316
40(Optimal)	2.0454×10^{-2}	5.0948×10^{-6}	2.0459×10^{-2}	464
60(Optimal)	1.0670×10^{-2}	1.0276×10^{-6}	1.0671×10^{-2}	363

aforementioned shaping and drain conditions.

Table 3 summarizes the execution status of the optimization runs carried out in this study. J_x denotes the first term in the objective function of equation 1 and J_T represents the second term evaluated with all the weights r_j fixed at 1.0. The first row lists the values of objective functions for the pilot cure steps shown in Fig. 3, and the other rows list those for the cure steps optimized with different sets of curing time.

Fig. 5(a) compares the pilot cure steps with the optimal cure steps for the same curing time of 50min, and Fig. 5(b) compares the respective final states of cure at the observation points numbered from the bladder side in each section of the tire. Except for an initial 10 minute period, the optimal cure steps show much lower temperature profile than the pilot steps. The optimized profile led to a higher SOC profile in each section than the pilot steps in Fig. 5(b) and accordingly to a smaller J_x value in Table 3. The difference in the SOC values between two cure steps is more salient at the observation points near the bladder than the mold side observation points because only the bladder side cure steps were optimized in this study. The lower SOC values for the pilot steps resulted from the overcure caused by the excessively high temperature profile of bladder side cure media. Besides the lower SOC values, the pilot steps must have caused the heat-sensitive layers to violate

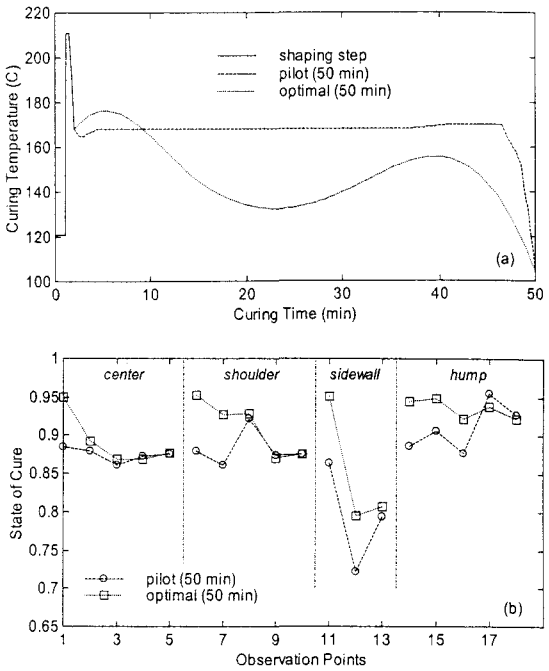

Fig. 5. Comparison of pilot vs. optimal cure steps (a) Temperature profiles of the bladder side cure media, (b) Final states of cure at the SOC observation points.

the respective temperature limits to a considerable degree as manifested by the much larger value of J_T in Table 3.

Fig. 6 shows the effect of the curing time on the optimal cure steps. When the mold was opened ten minutes earlier than the nominal case, the optimal temperature showed sharp increase as expected in order to prevent the undercure of rubber compounds. Although this elevated temperature of

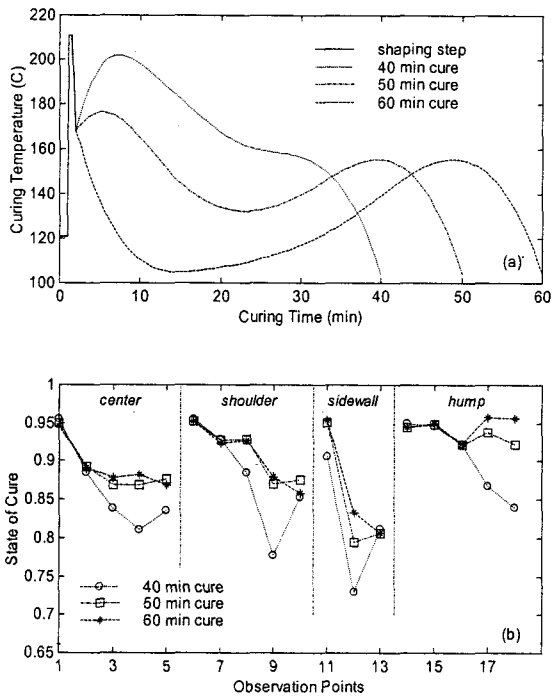

Fig. 6. Effect of curing time in optimal curing of the tire (a) Temperature profiles of the bladder side cure media, (b) Final states of cure at the SOC observation points.

bladder side cure media helped the adjacent layers to reach SOC levels comparable to those obtained at longer cure time, the innermost or mold side layers suffered from undercure due to insufficient curing time. When the mold opening time was prolonged to 60 minutes, the optimal cure steps showed initial decrease until about 15 min followed by a gradual peak. The lower curing temperature for longer time was necessary to prevent the overcure and, in fact, was more favorable to higher states of cure as manifested by smaller J_x values in Table 3 and higher SOC profiles in Fig. 6 (b). It should be noted, however, that longer cure time means decreased productivity, hence tradeoffs should be made between product quality and productivity.

VI. Conclusions

A systematic procedure was presented to determine optimal cure steps for product quality in a tire curing process. First, the product quality was formulated into an objective function that measures the deviation of final states of cure from the target values and the violation of temperature limits prescribed for heat-sensitive composite layers. Then, the objective function was minimized under an equality constraint representing the process model and under inequality constraints representing the operational temperature limits of cure media. Next, the time-varying profile of cure media temperature was discretized using B-splines. The resulting dynamic optimization problem was solved using a complex algorithm along with a finite element model solver. Finally, numerical simulation results were presented to demonstrate the procedure of determining the optimal cure steps for a tire.

References

1. W. J. Toth, J. P. Chang, C. Zanichelli, *Tire Science and Technology*, **19**, 178 (1991).
2. C. de Boor, "A Practical Guide to Splines", Springer-Verlag, 1978.
3. J. P. Holman, "Heat Transfer", 5th ed., McGraw-Hill, New York, 1981.
4. I.-S. Han, C.-B. Chung, and J.-W. Lee, *Rubber Chem. Tech.*, in press (1999).
5. L. S. Pontryagin, V. G. Gamkrelidze, and E. F. Mishenko, "The Mathematical Theory of Opti-

mal Processes", translated by D. E. Brown, Macmillian, New York, 1964.
6. E. B. Becker, G. F. Carey, and J. T. Oden, "Finite Elements. Volume I : An Introduction", Prentice Hall, New Jersey, 1981.
7. M. E. Davis, "Numerical Methods and Modeling for Chemical Engineers", John Wiley & Sons, New York, 1984.
8. I.-S. Han, C.-B. Chung, J.-H. Kim, S.-J. Kim, H.-C. Chung, C.-T. Cho, and S.-C. Oh, *Tire Science and Technology,* **24**, 50 (1996).
9. S. S. Rao, "Engineering Optimization : Theory and Practice", 3rd ed., John Wiley & Sons, New York, 1996.
10. B. M. Averick, R. G. Carter, and J. J. More, *MINPACK-2 Project,* Argonne National Laboratory and University of Minnesota, 1995.